

# Resolved 24.5 $\mu\text{m}$ Observations of Massive Young Stellar Objects

W. J. de Wit<sup>1</sup>, M. G. Hoare<sup>1</sup>, T. Fujiyoshi<sup>2</sup>, and R. D. Oudmaijer<sup>1</sup>

<sup>1</sup>School of Physics and Astronomy, University of Leeds, Leeds, LS2 9JT, UK

<sup>2</sup>Subaru Telescope, NAOJ, National Institute of Natural Sciences, 650 North A'ohoku Place, Hilo, HI 96720, USA

## Context and aims

The early stages in the lives of massive stars are identified by highly luminous ( $>10^4 L_{\text{sun}}$ ) yet very cool objects deeply embedded in their natal molecular cloud. These massive young stellar objects are surrounded by massive dusty envelopes, whose physical structure and geometry are determined by the star formation process. The aim of this poster is to establish the density structure of MYSO envelopes on scales of approximately 1000 AU. This constitutes an increase of a factor 10 in angular resolution compared to similar studies performed with single-dish telescopes in the (sub)mm. We have obtained diffraction-limited (0.6") 24.5  $\mu\text{m}$  images of 14 well-known massive star formation regions with the COMICS instrument on Subaru (Fig. 1). We construct azimuthally averaged intensity profiles of the resolved MYSO protostellar envelopes and build spectral energy distributions (SEDs) from archival data and COMICS fluxes. The SEDs range from near-infrared to the millimeter wavelength. Self-consistent 1-D dust radiative transfer models described by a density dependence of the form  $\rho(r) \sim r^{-p}$  are then used to simultaneously compare the 24.5  $\mu\text{m}$  intensity profiles and SEDs to model predictions (Fig. 4).

## 1. COMICS 24.5 $\mu\text{m}$ images

The 24.5  $\mu\text{m}$  images (see Fig. 1) reveal that all principal MYSO sources in the 14 targeted massive star forming regions are resolved. The sources are generally discrete and have fairly simple, circular morphologies on the sky suggesting that the emission is dominated by the circumstellar envelope rather than e.g. outflow cavities, warranting initial simple modelling with 1-D spherical radiative transfer codes.

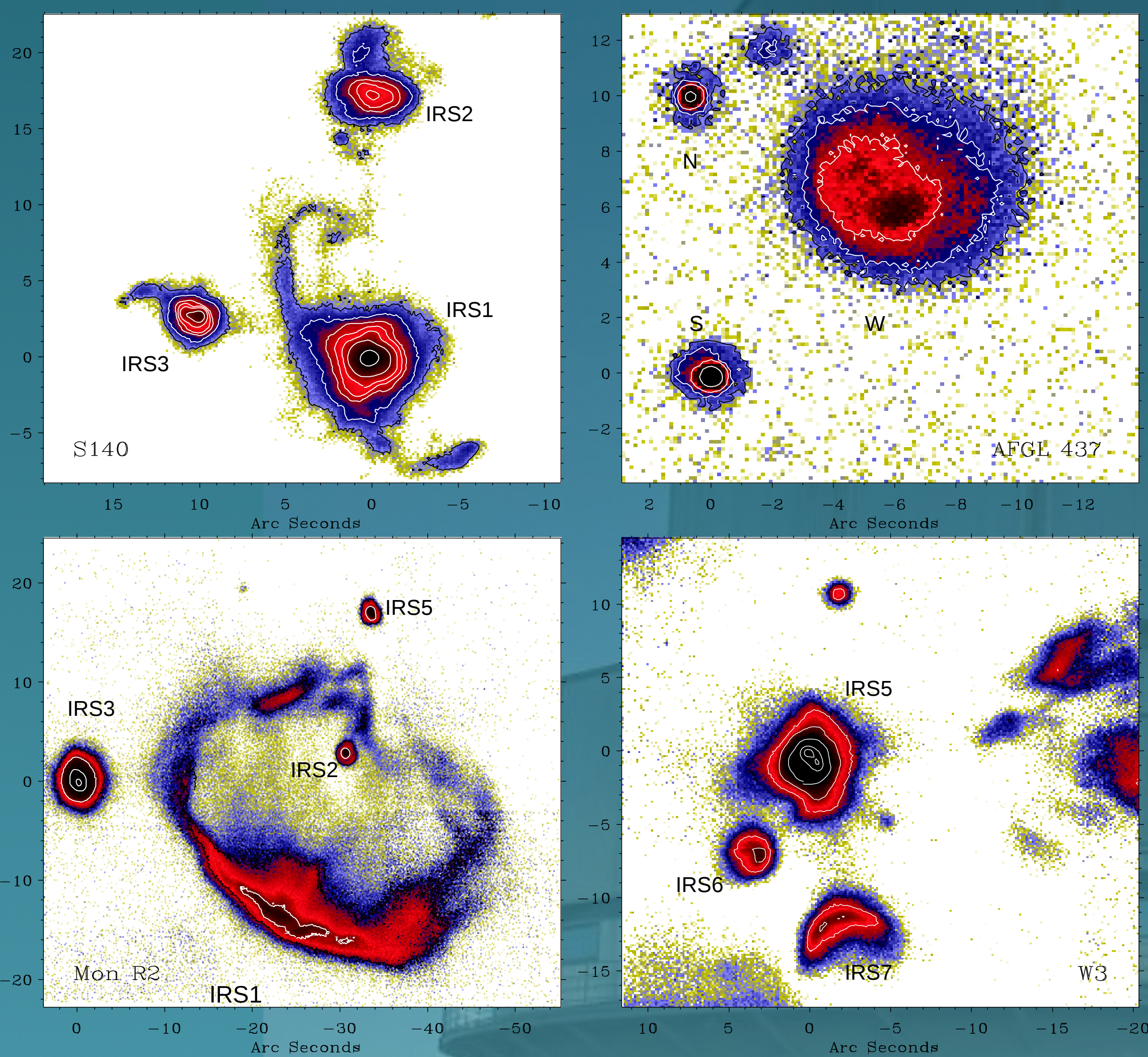
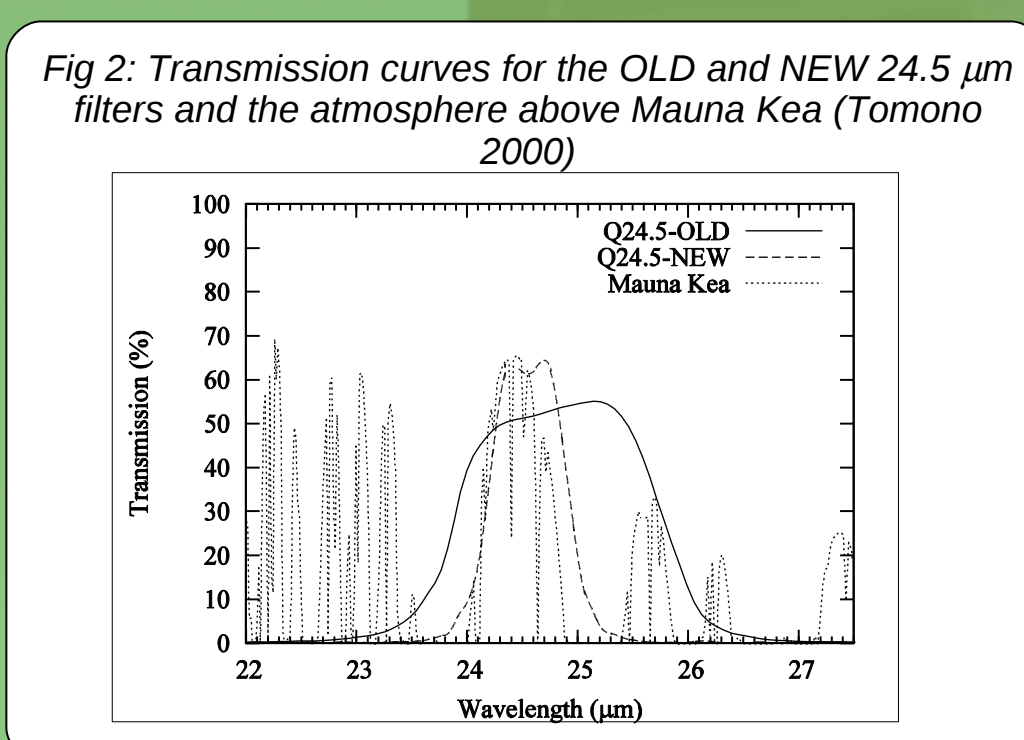


Fig. 1: Linearly scaled COMICS images of 4 massive star forming regions. Compact sources are MYSOs. Extended emission (e.g. AFGL 437W, Mon R2 IRS1) is associated with UC HII regions. The images also reveal a more diffuse component particularly visible in the S140 and Mon R2 regions.

## Technical intermezzo: Filters and PSF standards



**A.** Our COMICS images were taken with two different filters (Fig.2) over the course of the observations. The Q24.5-NEW filter makes an excellent fit to the small atmospheric window at 24.5  $\mu\text{m}$ , allowing the whole 40" x 30" Si:As IBS array to be read out.

**B.** Three of the six observed flux standards show evidence for extended emission (Fig. 3). These are  $\mu$  Cep,  $\alpha$  Her and  $\alpha$  Sco. Detailed analysis of the nebula of  $\mu$  Cep reveals an a-spherical distribution at sub arcsecond scales, suggestive of a preferred axis for the present-day mass loss of this red supergiant star (e.g. de Wit et al. 2008).

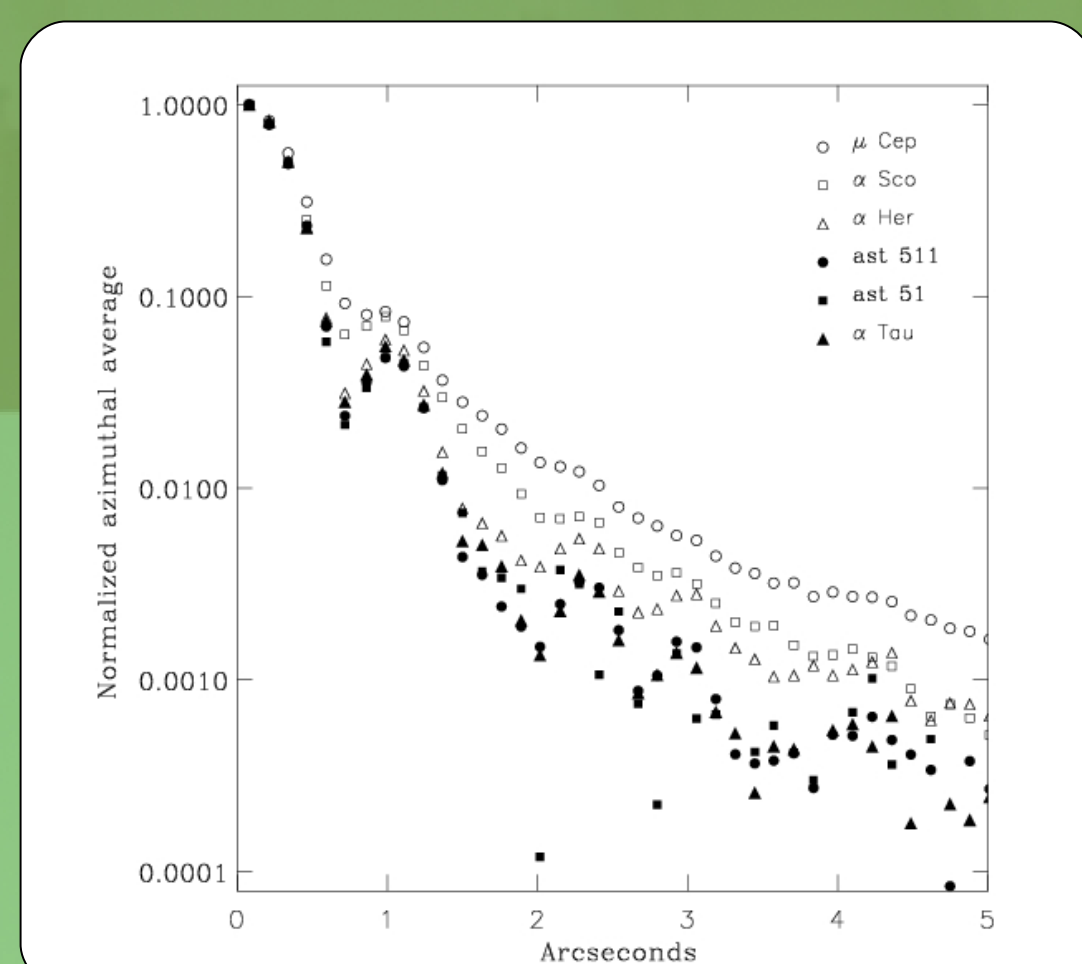


Fig. 3: Intensity profiles of observed standard stars tested for suitability as point spread function standards. Stars represented by open symbols are clearly surrounded by extended envelopes.

## Conclusions

For many sources, spherical models are capable of satisfactorily reproducing the 24.5  $\mu\text{m}$  intensity profile and flux density, the silicate feature, and the submm emission (e.g. S140 IRS1 in Fig. 4). They are described by density distributions of  $p=1.0$ . Such distributions are shallower than those found on larger scales. Other sources have density laws that are shallower/steeper than  $p=1.0$ , and there is evidence that they are viewed near edge-on or near face-on. In these cases spherical models fail to provide a good fit, as expected (e.g. M8E-IR in Fig. 4).

The analytic TSC solution for a freely infalling and rotating protostellar envelope (Tereby, Shu & Cassen 1984) predicts a transition from a  $p=1.5$  to a  $p=0.5$  density law at the so-called centrifugal radius. The latter depends on the total angular momentum of the envelope. The observed flattening of the density law from  $\sim 10\,000$  AU (as measured in the submm) to 1000 AU as presented here, could be the manifestation of increased rotational support of the infalling envelope.

## 2. SED and profile modelling

Model SEDs and images are calculated using DUSTY (Ivezic & Elitzur 1997). We use a spherically symmetric dust distribution illuminated by a central unresolved star. Total extinction (total envelope mass) is constrained by the observed 9.7  $\mu\text{m}$  silicate absorption for each target object. The required data were in most cases provided by ISO-SWS spectra. Infrared and (sub)mm data are taken from the literature, in 3 out of the 14 cases Spitzer MIPS photometry was available.

In order to perform a systematic comparison we generated a standard grid of 120 000 DUSTY models comprising different density profiles, dust mixtures, envelopes sizes and extinction. The subsequent fitting procedure takes into account the silicate feature, the continuum slope of the ISO-SWS spectra, the SED peak, and the (sub)mm continuum data. At the same time a fit is performed to the observed DUSTY azimuthally averaged COMICS intensity profile (see Fig. 4).

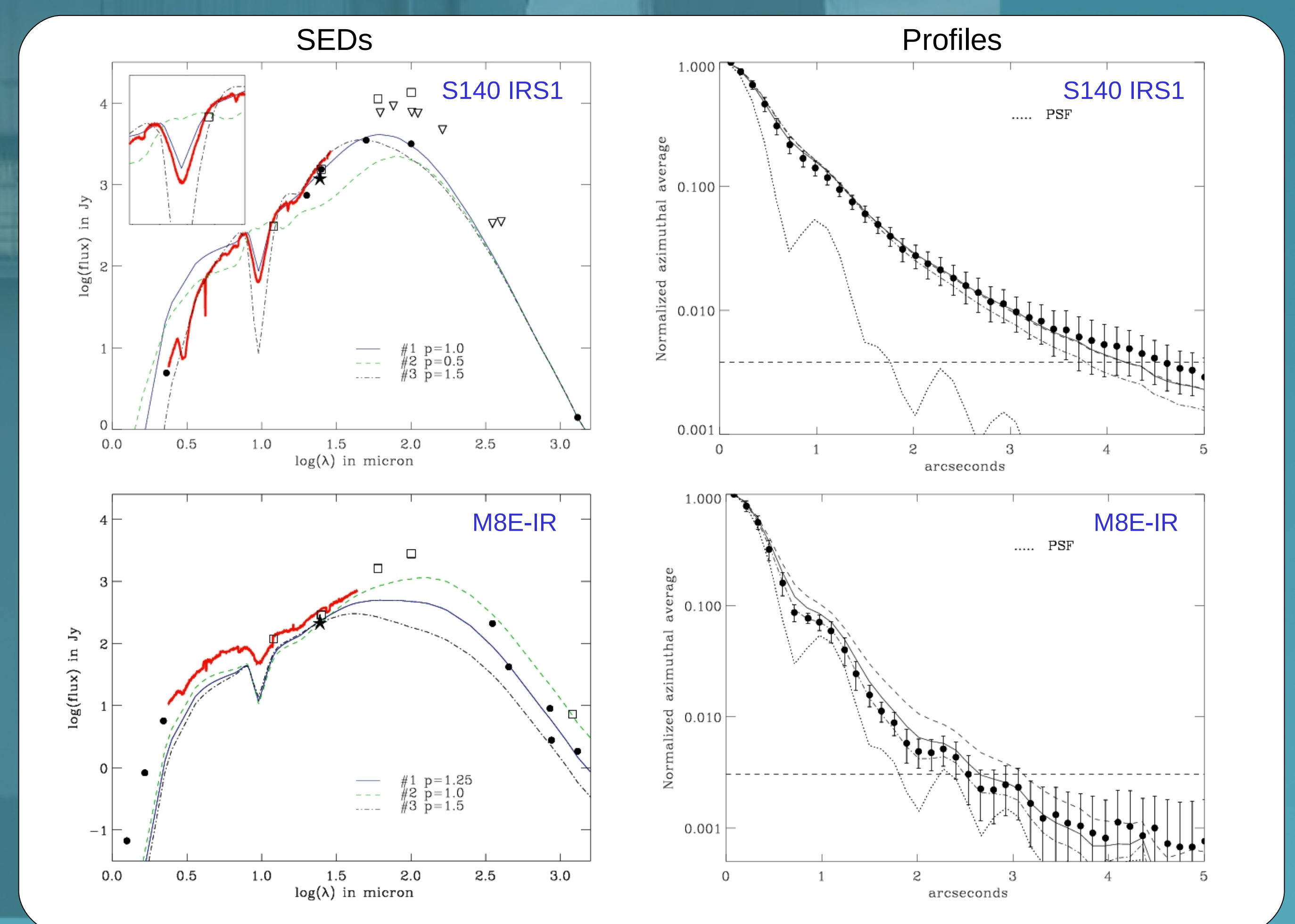


Fig. 4: Two examples of simultaneous SED (left panels) and azimuthally averaged intensity profile (right panels) fit. Shown are S140 IRS1 (upper panels) and M8E-IR (lower panels). Each panel shows three DUSTY models; the line style code is the same in each panel. Best fitting model is given by the full line. Density laws bracketing the best fits are also shown. Only data represented by filled symbols are fit; open symbols are large aperture measurements. COMICS flux density is represented by an asterisk. The fit to S140 IRS1 is considered a satisfactory fit, the fit to M8E-IR is not. The latter example illustrates the tendency to obtain steeper/shallower than  $p=1.0$  density laws, when the models fit poorly.

## Acknowledgements

We are grateful for financial support from the UK/Gemini support group. RDO acknowledges support from the Leverhulme Trust.

## References

de Wit, W. J., Oudmaijer, R. D., Fujiyoshi, T. et al. ApJ, 685, L75  
Tomono, D. 2000, PhD Thesis, University of Tokyo  
Tereby, S., Shu, F. H. & Cassen, P. 1984, ApJ, 286, 529  
Ivezic, Z. & Elitzur, M. 1997, MNRAS, 287, 7992